Journal of Alloys and Compounds 891 (2021) 162058

Contents lists available at ScienceDirect

Journal of Alloys and Compounds

journal homepage: www.elsevier.com/locate/jalcom

Surface modification on copper particles toward graphene reinforced copper matrix composites for electrical engineering application

Shengcheng Shu[a,b,c], Qiang Zhang[d], Joerg Ihde[b], Qilong Yuan[a], Wen Dai[a], Mingliang Wu[a], Dan Dai[a], Ke Yang[a], Bo Wang[a], Chen Xue[a], Hongbing Ma[a], Xu Zhang[e], Jiemin Han[f], Xuyuan Chen[g], Cheng-Te Lin[a,c,*], Wanbin Ren[e,**], Yifei Ma[f,**], Nan Jiang[a,c,*]

[a] Key Laboratory of Marine Materials and Related Technologies, Zhejiang Key Laboratory of Marine Materials and Protective Technologies, Ningbo Institute of Materials Technology and Engineering (NIMTE), Chinese Academy of Sciences, Ningbo 315201, China
[b] Fraunhofer Institute for Manufacturing Technology and Advanced Materials IFAM, Bremen 28359, Germany
[c] Center of Materials Science and Optoelectronics Engineering, University of Chinese Academy of Sciences, Beijing 100049, China
[d] Key Laboratory of Interface Science and Engineering in Advanced Materials, Ministry of Education, Taiyuan University of Technology, Taiyuan 030024, China
[e] School of Electrical Engineering and Automation, Harbin Institute of Technology, Harbin 150001, China
[f] State Key Laboratory of Quantum Optics and Quantum Optics Devices, Institute of Laser Spectroscopy, Collaborative Innovation Center of Extreme Optics, Shanxi University, Taiyuan 030006, China
[g] Faculty of Technology, Natural Sciences and Maritime Sciences, Department of Microsystems, University of Southeast Norway, Borre N-3184, Norway

ARTICLE INFO

Article history:
Received 22 July 2021
Received in revised form 6 September 2021
Accepted 18 September 2021
Available online 22 September 2021

Keywords:
Graphene nanoplatelet
Copper matrix composite
Surface modification

ABSTRACT

Graphene has been demonstrated as an effective reinforcement for metal matrix composites, due to its excellent mechanical properties, robust chemical inertness, thermal stability, and self-lubricating. Nevertheless, the limiting factor for its further use in metal matrix composites, is to realize the homogeneous dispersion of graphene for taking advantage of its exceptional and fascinating properties, because of the poor wettability and density contrast between metal matrix and graphene. Herein, we design a gel-assisted route to synthesize high-quality graphene nanoplatelets modified monodispersed copper particles, followed by hot pressing to fabricate graphene reinforced copper matrix composites bulk. This simple route with high efficiency and low cost, offers a new solution for the mass-production of graphene reinforced copper matrix composites and other graphene-based composites on an industrial scale. Significantly enhanced tensile strength of 253 MPa, and yield strength of 145 MPa, accompanied by the low friction coefficient and improved wear resistance, can be simultaneously achieved in the composites. For the real electrical contact performance test, the service life of electrical contacts made of graphene reinforced copper matrix composites, is 10 times longer as that of the commercial pure copper electrical contacts and almost comparable to CuAg20 contacts, demonstrating its superior ability to solve the electrical contact issues in electrical engineering systems.

1. Introduction

Graphene, composed of two-dimensional sp^2-hybridized carbon atoms, has been recognized as an effective reinforcement in metal matrix composites, owing to the exceptional chemical inertness, electron mobility, self-lubricating performance and mechanical properties [1–5]. However, graphene is difficult to be homogeneously dispersed in the copper matrix, due to the agglomeration driven by the Van der Waals force and the density contrast between copper matrix (8.9 g cm^{-3}) and graphene (2.2 g cm^{-3}) [6,7]. Beyond that, poor wettability between graphene and metallic matrix raises the difficulty level to achieve a homogeneous dispersion [8]. In addition, the adhesion between graphene sheets and copper matrix is limited to Van der Waals interaction, which weakens the performance of graphene sheet reinforced copper matrix composites [8–10]. Therefore, the key issue to obtain higher reinforcing efficiency of graphene in copper matrix composites lies in the advanced

* Corresponding authors at: Key Laboratory of Marine Materials and Related Technologies, Zhejiang Key Laboratory of Marine Materials and Protective Technologies, Ningbo Institute of Materials Technology and Engineering (NIMTE), Chinese Academy of Sciences, Ningbo 315201, China
** Corresponding authors.
E-mail addresses: linzhengde@nimte.ac.cn (C.-T. Lin), renwanbin@hit.edu.cn (W. Ren), mayifei@sxu.edu.cn (Y. Ma), jiangnan@nimte.ac.cn (N. Jiang).

https://doi.org/10.1016/j.jallcom.2021.162058
0925-8388/

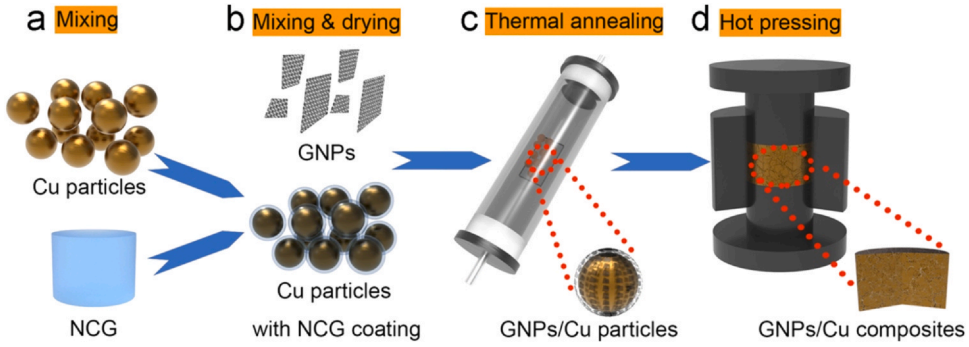

Fig. 1. Schematic illustration of the synthesis route for GNPs/Cu composites.

architecture design combining the homogeneous dispersion, strong interfacial bonding and stable structure of the composites.

During the past decades, several effective synthesis methods, such as mechanical ball milling, molecular-level mixing (MLM), in-situ chemical vapor deposition (CVD), have been developed to disperse graphene homogeneously and obtain tight interfacial bonding between graphene and copper matrix, for improving the performance of graphene reinforced copper matrix composites [4,11–17]. Dong et al. introduced a plasma-assisted ball milling method to fabricate graphene/copper composites with an enhanced tensile strength of 260 MPa [11]. However, the high energy during ball milling process may lead to the structural defects of graphene and exert a negative impact on the intrinsic electrical conductivity of the composites. Hwang et al. developed an MLM and a following spark plasma sintering (SPS) process for homogeneous distribution of reduced graphene oxide (RGO) in copper matrix composites [4]. They demonstrated that the Cu-O-C bonding at the grain boundary of RGO/copper nanocomposites can efficiently improve the tensile strength and elastic. It is noteworthy that mass of defects introduced from MLM process may remarkably bring down the intrinsic thermal diffusion and electrical conductivity of copper matrix, which results from the heavy use of strong acids and bases for pre-treatment of graphene via Hummers' method. Compared with ball milling and MLM routes, the in-situ CVD method has been demonstrated as an effective method to obtain a homogeneous dispersion of graphene in copper matrix as well as tight interfacial bonding between graphene coating and copper particles. However, copper particles would be melted and aggregated owing to the high temperature during CVD procedure, which approximates the melting point of copper (1084 °C) [15,18]. Therefore, graphitic spacer particles have to be used during the coating process, or the deposition temperature have to be reduced which may give rise to defects density of graphene, by reason of the self-limited growth mechanism of graphene on copper matrix during the CVD procedure [19–21]. An alternative approach by using an inline atmospheric pressure plasma CVD coating process has been shown promising results instead of batch CVD processes, but the mechanical performance of the achieved graphene-like carbon reinforced copper composites still needs to be improved [6]. Therefore, an urgent need exists to develop efficient and scalable methods to achieve advanced graphene reinforced copper matrix composites with homogeneous dispersion of high-quality graphene.

In this work, we propose a gel-assisted milling method for the synthesis of high-quality graphene nanoplatelets (GNPs) modified monodispersed copper particles, followed by vacuum hot pressing to fabricate GNPs reinforced copper matrix (GNPs/Cu) composites, which is high-efficiency compared with the reported methods and facilitates mass production on an industrial scale. Comparing to pristine copper, the GNPs/Cu composites demonstrate enhanced tensile strength of 253 MPa, yield strength of 145 MPa, lower friction coefficient and improved wear resistance simultaneously. During the real electrical contact performance test, the service life of our GNPs reinforced copper matrix composites as electrical contacts is 10 times longer than that of the commercial pure copper electrical contacts, demonstrating the superior ability to solve the electrical contact issues in electrical engineering systems.

2. Materials and methods

2.1. Materials

The spherical copper particles with a diameter (D50) of 20 μm were purchased from Shanghai Shuitian Nanotechnology Co., Ltd. The 0.65% nanocellulose gel (NCG) was provided by Guilin Qihong Tech. Co., Ltd. GNPs were produced by Ningbo Morsh Tech. Co., Ltd. The commercial pure copper electrical contacts were supported by State Grid Co., Ltd.

2.2. Synthesis of GNPs encapsulated monodispersed copper particles

As shown in Fig. 1a, 20 g spherical copper particles were mixed with 2 g 0.65% NCG via a high-speed mixer (DAC 150, FlackTek Ltd., Germany) with a rotation speed at 3500 r/min. After the mixing process, the copper particles are homogeneously coated by NCG. In Fig. 1b, 0.5 g GNPs were mixed with the copper particles with NCG coating via a high-speed mixer with a rotation speed at 3500 r/min. Due to the adhesion of NCG, the GNPs can be affixed on copper particles. After vacuum evaporation of water at 60 °C for 2 h, the as-prepared particles are loaded into a quartz tube, which was heated to 800 °C at a heating rate of 15 °C min^{-1} with 100 sccm Ar flow and 30 sccm H_2 flow (Fig. 1c). The annealing process was kept at 850 °C for 2 h under the Ar (100 sccm) and H_2 (30 sccm) flow, followed by rapidly cooling down with a rate of 35 °C min^{-1}. At last, the as-prepared GNPs/Cu particles were passed through vibrating screen of 5000 meshes for removal of redundant GNPs, which are separated from the GNPs/Cu composite particles.

2.3. Hot pressing sintering of GNPs/Cu composite bulk

The GNPs/Cu composite particles were set into a graphite mold with diameter of 20.0 mm and then were hot pressed into bulk under a pressure of 40 MPa at 850 °C for 20 min with a vacuum of 10 Pa level. The heating rate was maintained at 25 °C min^{-1}. In the final hot pressing process, sintering parameters such as imposed pressure, holding pressure and temperature, would be of vital importance on the construction of homogeneous and continuous graphene framework with copper matrix. The GNPs/Cu composite bulk was polished by 80, 500, 1200, 2400, and 5000 mesh Al_2O_3 waterproof abrasive papers in sequence. The thickness of GNPs/Cu bulk

was polished to about 6 mm. A counterpart pure copper bulk was also fabricated by the same parameter.

2.4. Characterization

The morphologies of the samples were observed utilizing field emission scanning electron microscope with electron back-scattered diffraction (EBSD) (SEM, Verios G4 UC, Thermo Scientific, USA) and 3D Surface Scanning System (UP-Lambda, Rtec, USA). Raman spectrometer (Renishaw inVia Reflex, Renishaw, UK) with a laser wavelength of 532 nm was adopted to analyze the defects of graphene. The crystal structure and composition of the composites were analyzed by X-ray diffraction (XRD, Bruker D8 Advance, Bruker, Germany). High frequency infrared carbon/sulfur element analysis system (CS844, LECO, USA) was utilized to measure the content of GNPs within the composites. Transmission electron microscope (TEM, Talos F200x, ThemoFisher, USA) were utilized to characterize the microstructures of GNPs as well as GNPs/Cu composites. The thickness of GNPs was determined by atomic force microscopy (AFM, Dimension 3100, Vecco, USA).

Tensile stress-strain curves of the GNPs/Cu composites and pure copper samples were measured by electronic universal testing machine (5569 A, Instron, USA) with a speed of 0.5 mm min^{-1}under ambient condition. Dog-bone shaped samples were prepared by wire-cut for tensile strength measurement. The gauge length, width and thickness were 10 mm, 2 mm, 1 mm, respectively. A multifunctional tribometer (UMT3, CETR, USA) was used for friction tests in ambient air. The setting mode of friction tests was reciprocating ball-on-disk and sliding against GGr15 steel balls with a diameter of 3 mm. The sliding speed and load force were 0.5 mm s^{-1}, 10 N, lasted for 1800 s. The length of the wear track was 0.5 mm. The hardness values were measured by a Vickers hardness tester (HX-1000TM, Shanghai Optical, China).

The electrical contact performance tests were carried out on an electrical contact tester. The parameters of the test are listed in Table S1. The service life, electrical contact resistance, arc energy, contact force and welding force are automatically measured by the electrical contact tester. All tested samples have been cut in cylindrical specimens with 3 mm in diameter, 5 mm in height, and have been polished as described above.

3. Results and discussion

The main task for obtaining advanced graphene reinforced copper matrix composites, is to construct the homogeneous coating of graphene on the surface of copper particles and a homogeneous graphene framework within copper matrix composite bulk. In our strategy, we propose a gel-assisted milling method, which starts from defined coating with GNPs on the surface of spherical copper particles by speed mixing and thermal annealing. Fig. 1 indicates the overall synthesis route of GNPs/Cu composites, which can be mainly divided into four steps. The construction of homogeneous and continuous framework can be attributed to special sheet welding mechanisms, which has been demonstrated in the reported studies [22–24].

As shown in Figs. 2a, S1 and S2, the particle size of pure copper particles ranges from 5 to 35 μm in diameter with the average particle size of about 21 μm. Due to the adhesion of NCG, the GNPs can be affixed on pre-coated copper particles, which is essential to achieve a homogeneous dispersion of GNPs in the copper matrix. Fig. 2b exhibits the morphology of an individual GNPs/Cu particle after the gel-assisted milling and thermal annealing process. The morphology of separated spherical copper particles modified by GNPs could be obviously identified. After thermal annealing temperature of 800 °C, the agglomeration between GNPs/Cu particles could be fully avoided and a loosely-packed-sphere shaped particles could be maintained well. After the thermal annealing process for evaporation of NCG, GNPs/Cu composite particles can be obtained with tight interfacial bonding between copper matrix and GNPs. The AFM image in Fig. 2c and corresponding height-distance curve in Fig. S3 indicate the GNPS with a diameter of several micrometers are not agglomerated and have a typical thickness of ≈5 nm, suggesting the multilayer structure of GNPs. To further explore the morphologies and quality of GNPs coated on copper particles, the copper matrix is eliminated by using 0.5 M ammonium persulfate solution and the GNPs are observed by TEM. In Fig. 2d, some typical wrinkles of GNPs are distinguishable in the TEM image and the high transparency of the graphene can be clearly seen due to its ultrathin structure. From the HRTEM image in Fig. 2e, about 15 layers of graphene are countable at the edge of GNPs. The selected area electron diffraction (SAED) pattern in Fig. 2f shows strong diffraction spots with a well-defined hexagonal structure, indicating high crystallinity of GNPs [25]. In order to better characterize the defects and crystallinity of the GNPs, the Raman spectrum of GNPs/Cu particles is presented in Fig. 2g, in which three typical peaks of graphene related to the D-band (~ 1345 cm^{-1}), G-band (~ 1572 cm^{-1}), and 2D-band (~ 2708 cm^{-1}) can be found. In Fig. 2g, a weak D-band can be found with a calculated I_D/I_G ratio of 0.14, suggesting the a quite low defect level and high crystallinity, which is consistent with the SAED observation in Fig. 2f as well as the XRD pattern in Fig. S4 [26]. In terms of high frequency infrared C-S analysis, the load content of GNPs in GNPs/Cu composites is about 0.5 wt%, while the carbon content in the pure copper sample is merely 0.01 wt%. As a result, GNPs/Cu composites with low content of homogeneous low-defect graphene can be reliably synthesized using gel-assisted milling and sintering by hot pressing.

The representative engineering stress-strain curves and comparative tensile properties of the pure copper and GNPs/Cu composites are presented in Fig. 3a and b, which is indicative of the ultimate tensile strengths of GNPs/Cu composites (253 MPa) are almost 19% higher than that of the pure copper samples (212 MPa). Besides, the GNPs/Cu composites deliver a yield strength of 145 MPa, which is markedly superior to that of pure copper (85 MPa). The fractural elongation of GNPs/Cu composites is measured as 16.5%, which is as 54% less as that of pure copper. Fig. 3c exhibits the work hardening rate-true strain curve. Comparing to pure copper, the GNPs/Cu composites enhanced work hardening capacity and higher work hardening rate throughout almost entire probed strain range [27,28]. Based on the Considere criterion, while the work hardening rate increase, deformation resistance and dislocation storage rate would be enhanced, which is beneficial to the engineering tensile strength.

The interfacial bonding between graphene and copper matrix plays critical role in determining the mechanical properties of the composites [4]. To investigate the interfacial bonding between graphene and copper matrix, TEM and related inverse Fourier-filtered images are obtained. Fig. 3d and e show the HRTEM and inverse Fourier-filtered images near Cu-Cu boundary, demonstrating that limited dislocation accumulations near the Cu-Cu boundary in pure copper. As shown in Figs. 3f and S6b, continuous multilayer graphene can be observed at the grain boundary. No gaps or impurities could be found along the interface between graphene and copper matrix, which means tight interfacial bonding between graphene and copper. In Fig. 3g, the dislocation storage capacity at the Cu-graphene boundary in GNPs/Cu composites is significantly enhanced, leading to the improvement in tensile strength according to the dislocation strengthening mechanism [7,9,29]. The reason for enhanced dislocation density near the Cu-graphene boundary can be attributed to the wrinkles and layer thickness, which may be the origin of defects in the GNPs/Cu composites [2,11].

The shape and size of the matrix grain after hot pressing are identified by electron back-scattered diffraction (EBSD). As shown in

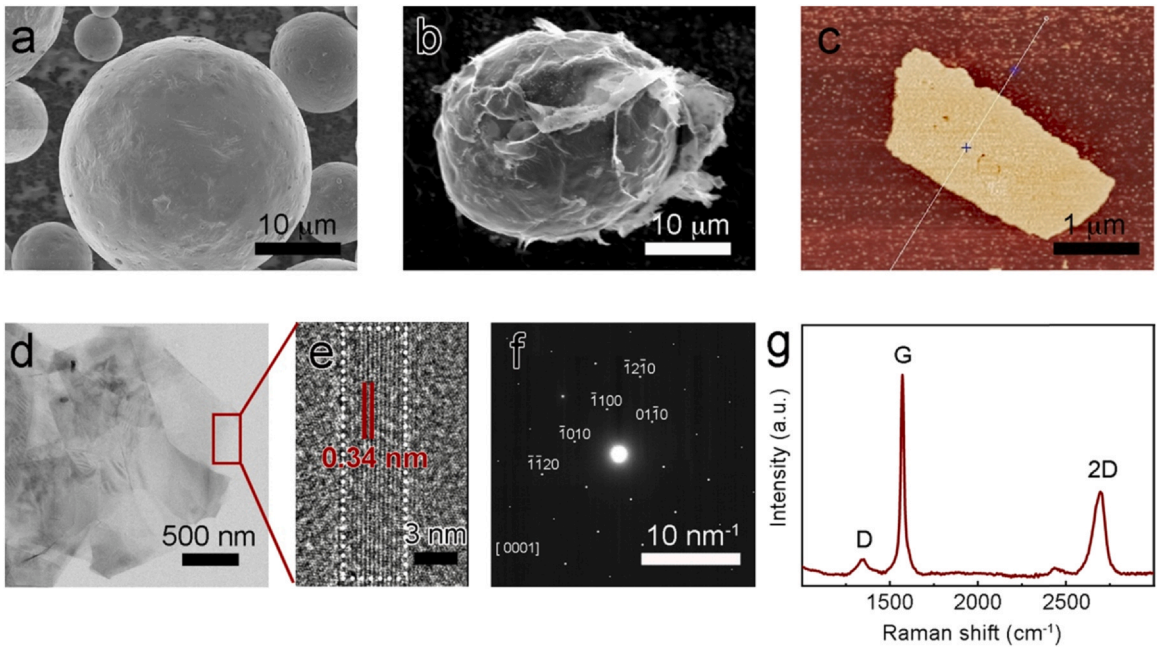

Fig. 2. Typical morphologies of (a) pure copper particles and (b) GNPs/Cu particles after thermal annealing. (c) Typical AFM image of GNP. (d) TEM image of GNPs. (e) Related HRTEM image, and (f) SAED pattern of the GNPs in (d). (g) Typical Raman spectrum of GNPs/Cu particles.

Fig. 4, both of the samples display irregular shapes, and the statistical result indicates that the average grain size of the GNPs/Cu (5.82 μm) is smaller than pure copper (8.24 μm). As shown in Fig. S5a and b, the graphene layers distributed along the grain boundaries and inhibit the grain growth, which possibly contributes to the enhancement of strength.

In consideration of the frequent circuit switching at the electrical contact point, low friction coefficient, intensive wear resistance and hardness are imperative for the real application of electrical contact materials. Fig. 5a shows the friction coefficient-sliding time curves of pure copper and GNPs/Cu composites measured under a contact pressure of 10 N for 1800 s. The friction coefficient of GNPs/Cu composites is about 0.27, which indicates a 65% reduction compared with that of pure copper (0.78). In Fig. 5b and c, the wear track of GNPs/Cu is obviously shallower depth and narrower width, than that of pure copper. On the basis of wear volume, the wear rates are calculated and summarized in Fig. 5d. The wear rate of GNPs/Cu composites is merely 3.9×10^{-4} mm^3 N^{-1} m^{-1}, which is one order of magnitude lower than that of pure copper (26×10^{-4} mm^3 N^{-1} m^{-1}). The hardness value of GNPs/Cu composites is measured to be 78 HV,

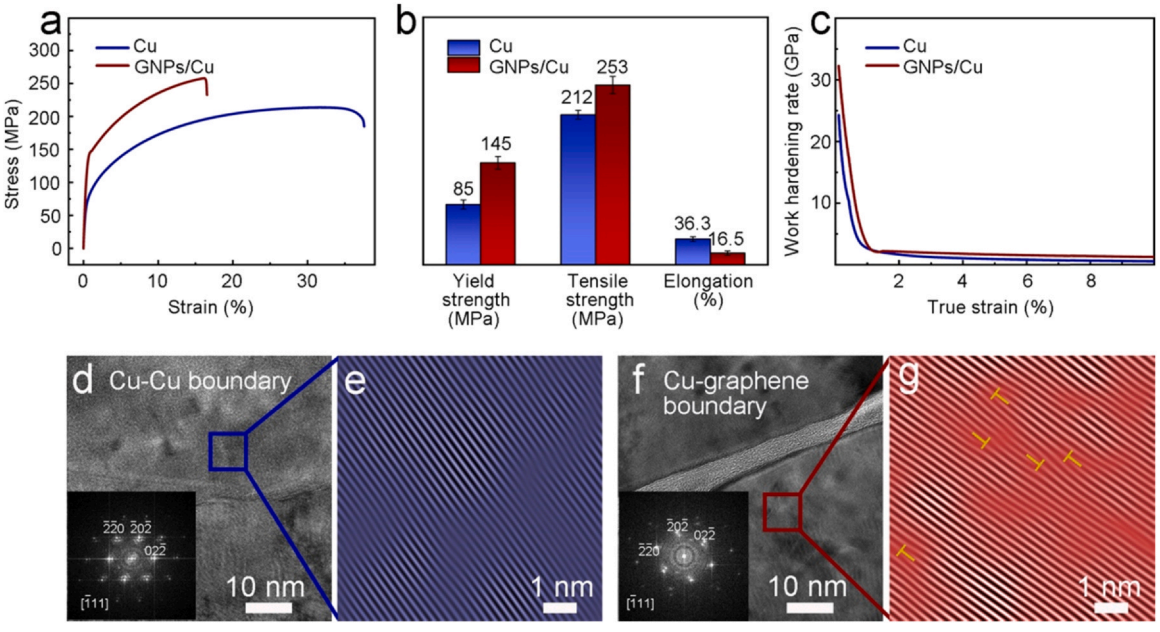

Fig. 3. (a) Engineering tensile stress-strain curves of pure copper and GNPs/Cu composites. (b) Tensile properties of pure copper and GNPs/Cu composites. (c) Work hardening rate-true strain curves of pure copper and GNPs/Cu composites. (d) HRTEM image close to the grain boundary in as-prepared pure copper bulk. The inset image shows the original Fourier transformed pattern from the selected area. (e) The inverse Fourier-filtered image from the selected area in (d). (f) HRTEM image near the Cu-graphene boundary in as-prepared GNPs/Cu composites. The inset image shows the original Fourier transformed pattern from the selected area. (g) The inverse Fourier-filtered image from the selected area in (f).

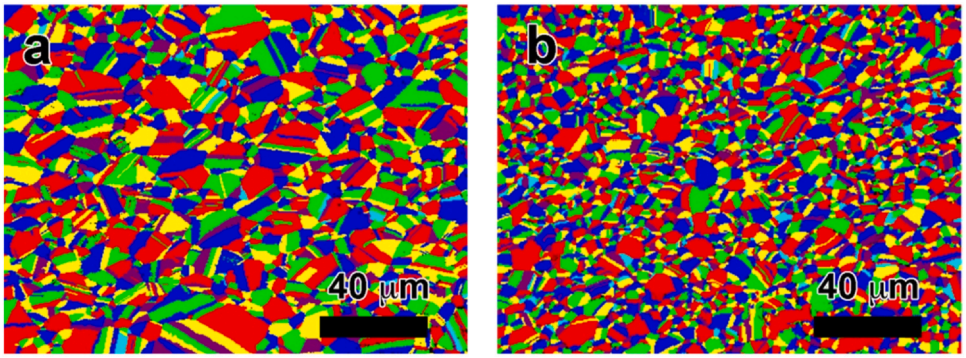

Fig. 4. EBSD micrographs of (a) pure copper and (b) GNPs /Cu composite bulk after hot pressing.

which shows 24% improvement than that of pure copper (63 HV). Clearly, the implementation of graphene can significantly decrease the friction coefficient and improve the wear resistance as well as hardness value of copper matrix composites.

To better understand the effect of GNPs on the friction properties of the composites, the surface morphologies of pure copper and GNPs/Cu are depicted in Fig. 5e and f after a sliding time for 800 s. As shown in Fig. 5e, the surface of pure copper is seriously worn and exhibits considerable peeling holes and increasing roughness. In Fig. 5f, the wear track of GNPs/Cu composites has not obvious peeling holes and is smoother than that of pure copper. In addition, some abrasive GNPs can be released and transferred on the surface of the GNPs/Cu wear track, which may further decrease the surface roughness as well as the wear rate of GNPs/Cu composites.

Based on the enhanced tensile strength of 253 MPa, yield strength of 145 MPa, and the intensive wear resistance, GNPs/Cu composites exhibit a great potential for electrical contact applications. Hence, we investigate the electrical contact properties of CNPs/Cu composites in a real electrical contact performance measurement exhibited in Video S1. Service life (operation number of on-off switching cycle) is the foremost target to evaluate the suitability and reliability of the composites applying as electrical contact. In Fig. 6a, the GNPs/Cu composites demonstrate 586 on-off switching cycles before failure, indicating 10 times longer service life than that of commercial pure copper electrical contact (58 cycles). As can be seen in Fig. 6b and c, the failure of commercial pure copper electrical contact can be attributed to the sharp increase of electrical contact resistance and contact force when the cycle number reaches the service life. In contrast, the electrical contact resistance and contact force of GNPs/Cu composites contact remain stable until the failure, suggesting the arc stability and oxidation resistance of GNPs/Cu composites. The failure reason for GNPs/Cu composite contact might be the increasing surface roughness caused by frequent arc. In Fig. 6d, the arc energy of GNPs/Cu composite contact steadily fluctuates around 2.0–2.5 J during the frequent on-off switching operations. As a result, the GNPs/Cu contact exhibits almost 10 times longer service life with stable electrical contact performance, comparing to that of commercial pure copper contact.

Supplementary material related to this article can be found online at doi:10.1016/j.jallcom.2021.162058.

The surface morphologies of commercial pure copper contact and our GNPs/Cu composite contact after frequent on-off operations are shown in Fig. 6e and f. The residual agglomeration of graphene with sharp edges in GNPs/Cu can be found in Fig. 6f and related EDS

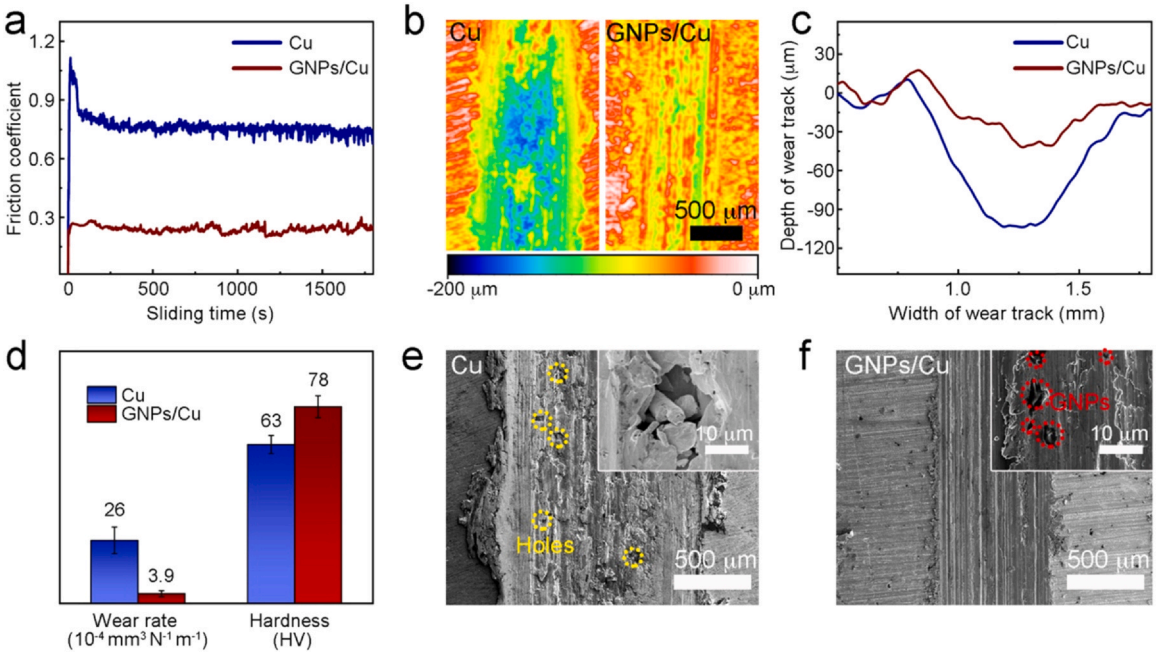

Fig. 5. (a) Friction coefficient of pure copper and GNPs/Cu composites. (b) The depth mapping of the wear tracks on pure copper and GNPs/Cu. (c) Corresponding wear track profiles of pure copper and GNPs/Cu composites. (d) Wear rates and hardness values of pure copper and GNPs/Cu composites. SEM images of the wear tracks on pure copper (e) and GNPs/Cu composites (f).

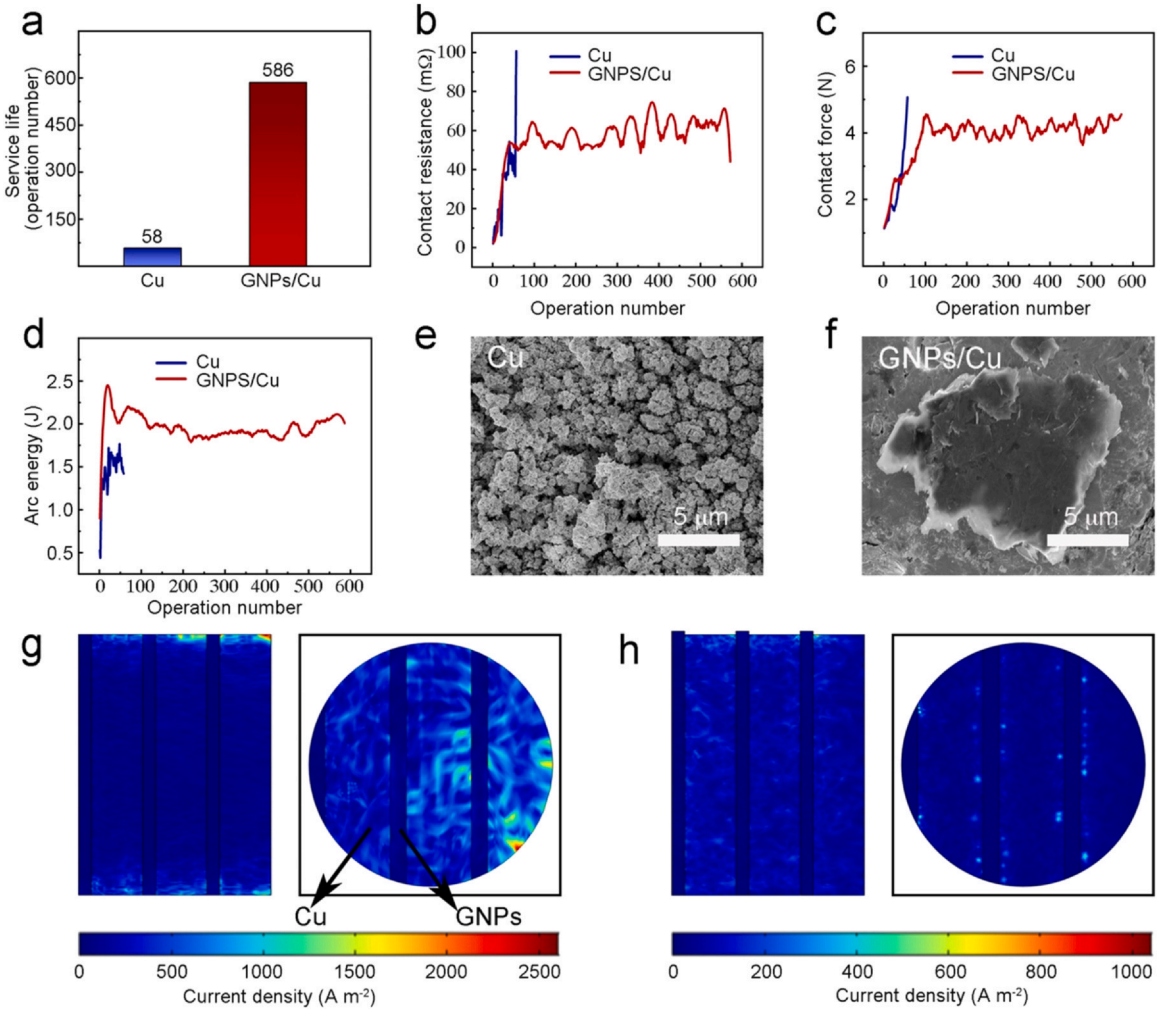

Fig. 6. (a) Comparison of service life between the commercial pure copper contact and GNPs/Cu contact in the electrical contact performance test. (b) Electrical contact resistance of the commercial pure copper contact and GNPs/Cu contact. (c) Contact force of the commercial pure copper contact and GNPs/Cu contact. (d) Arc energy of the commercial pure copper contact and GNPs/Cu contact. Surface morphology of (e) commercial pure copper contact and (f) GNPs/Cu contact after the electrical contact performance test. Simulation for current density distribution of sandwich structured GNPs/Cu (g) without sharp graphene edges and (h) with sharp edges on the top surface under the same applied arc voltage.

mapping in Fig. S6, owing to the high melting point and chemical inertness of graphene against arc ablation [30].

During arc ablation process, electrons escape from the surface of Cu and graphene. The density of escaped electrons can be calculated using Richardson-Dushman formula:

$$j = AT^2 e^{-\frac{\varnothing}{\kappa T}} \quad (1)$$

Where j is the density of electrons (eV/A); A is constant; T is the temperature (K); $\varnothing$ is the work function; κ is the thermal conductivity (W m^{-1} K^{-1}).

The work function (5.1 eV) and thermal conductivity (1900 W m^{-1} K^{-1}) of multilayer graphene are much higher than that of copper (4.5 eV, 407 W m^{-1} K^{-1}), which has been demonstrated in a number of studies [31–33]. Therefore, the electron density of Cu is higher than that of graphene, when the arc is generated on the surface of the composite. Owing to the lower work function and melting point, the region of copper in GNPs/Cu composites would be arc ablated and evaporated in prior to the region of graphene. After the evaporation of copper, residual graphene with sharp edges can work as lightning rods. Due to the lightning-rod effect of sharp graphene edge, the graphene can focus and consume the arc energy for the reduction of ablation and evaporation in the region of copper [34].

In order to further confirm the mechanism of graphene edges, finite-element simulations of current density distribution during arc plasma ablation in the structurally simplified GNPs/Cu composites, are processed utilizing COMSOL Multiphysics. Figs. 6g and S7 show the current density distribution of GNPs/Cu composites without sharp graphene edges on the top surface. The highest current density on the top surface is up to ~2300 A m^{-2}. Under the same applied voltage, the highest current density of GNPs/Cu composites with sharp graphene edges on the top surface is merely ~400 A m^{-2} in Fig. 6h and S8, indicating the exceptional protective effect of graphene edges during arc ablation process.

Cu-Ag alloy has been proved as the most common and reliable low-voltage electrical contact materials, owing to the low electrical contact resistance, excellent thermal conductivity, and high wear resistance. To further characterize the service performance of our GNPs/Cu composite, a comparative study was done by recording the service life of our samples and Cu-Ag alloys. All the parameters of service performance test are consistent with that in Table S1. Five batches of Cu-Ag alloys with Ag content of 1, 5, 10, 20, 30 wt%, are specified as CuAg1, CuAg5, CuAg10, CuAg20, CuAg30, respectively. As the results in Fig. 7 indicate, the service life of CNPs/Cu composite is almost comparable to that of CuAg20 and longer than that of

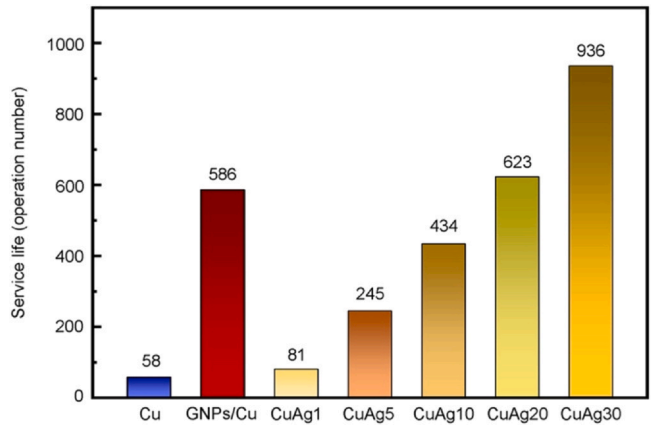

Fig. 7. A comparative service performance test for pure Cu, GNPs/Cu composite, and Cu-Ag alloys with varying Ag content.

CuAg10. This confirms the significant enhancement of service life of GNPs in copper matrix, which offers a probability to the consumption of Ag in electrical contact area.

4. Conclusion

In summary, we develop a scalable surface modification method for the synthesis of high-quality graphene nanoplatelets encapsulated monodispersed copper particles, followed by vacuum hot pressing to fabricate graphene reinforced copper matrix composites. Comparing to pure copper, the tensile strength and yield strength are enhanced by 19% and 71% respectively, owing to the enhanced dislocation density around Cu-graphene boundary. Besides, lower friction coefficient and enhanced wear resistance can be simultaneously achieved in our GNPs/Cu composites. In the real electrical contact performance test, due to the higher work function of graphene, the GNPs/Cu contact exhibits almost 10 times longer service life with stable electrical contact performance, comparing to that of commercial pure copper contacts, demonstrating GNPs/Cu composites a promising candidate for application as electrical contacts.

CRediT authorship contribution statement

Shengcheng Shu: Conceptualization, Methodology, Writing – original draft preparation. **Qiang Zhang:** Methodology, Writing – review & editing. **Joerg Ihde:** Writing – review & editing. **Qilong Yuan:** Data curation, Methodology. **Wen Dai**: Formal analysis. **Mingliang Wu:** Writing – review & editing. **Dan Dai:** Formal analysis. **Ke Yang:** Writing – review & editing. **Bo Wang:** Writing – review & editing. **Chen Xue:** Methodology. **Hongbing Ma:** Methodology. **Xu Zhang:** Methodology. **Jiemin han:** Data curation. **Xuyuan Chen:** Data curation. **Wanbin Ren:** Formal analysis. **Yifei Ma:** Formal analysis. **Cheng-Te Lin:** Supervision, Funding acquisition. **Nan Jiang:** Project administration.

Declaration of Competing Interest

The authors declare that they have no known competing financial interests or personal relationships that could have appeared to influence the work reported in this paper.

Acknowledgments

The authors are grateful for the financial support by the National Natural Science Foundation of China (U1709205), National Key R&D Program of China (2017YFB0406000 and 2017YFE0128600), the Project of the Chinese Academy of Sciences (XDC07030100, XDA22020602, KFZD-SW-409, ZDKYYQ20200001, and ZDRW-CN-2019–3), CAS Youth Innovation Promotion Association (2020301), Science and Technology Major Project of Ningbo (2018B10046 and 2016S1002), the Natural Science Foundation of Ningbo (2017A610010), Foundation of State Key Laboratory of Solid lubrication (LSL-1912), National Key Laboratory of Science and Technology on Advanced Composites in Special Environments (6142905192806), K.C. Wong Education Foundation (GJTD-2019–13), the 3315 Program of Ningbo and the joint doctoral promotion program of Fraunhofer-Gesellschaft and the Chinese Academy of Science (CAS) for financial support.

Appendix A. Supporting information

Supplementary data associated with this article can be found in the online version at doi:10.1016/j.jallcom.2021.162058.

References

[1] S. Chen, L. Brown, M. Levendorf, W. Cai, S.Y. Ju, J. Edgeworth, X. Li, C.W. Magnuson, A. Velamakanni, R.D. Piner, J. Kang, J. Park, R.S. Ruoff, Oxidation resistance of graphene-coated Cu and Cu/Ni alloy, ACS Nano 5 (2011) 1321–1327, https://doi.org/10.1021/nn103028d
[2] Z. Yang, L. Wang, Z. Shi, M. Wang, Y. Cui, B. Wei, S. Xu, Y. Zhu, W. Fei, Preparation mechanism of hierarchical layered structure of graphene/copper composite with ultrahigh tensile strength, Carbon 127 (2018) 329–339, https://doi.org/10.1016/j.carbon.2017.10.095
[3] A. Dorri Moghadam, E. Omrani, P.L. Menezes, P.K. Rohatgi, Mechanical and tribological properties of self-lubricating metal matrix nanocomposites reinforced by carbon nanotubes (CNTs) and graphene – a review, Compos. Part B Eng. 77 (2015) 402–420, https://doi.org/10.1016/j.compositesb.2015.03.014
[4] J. Hwang, T. Yoon, S.H. Jin, J. Lee, T.S. Kim, S.H. Hong, S. Jeon, Enhanced mechanical properties of graphene/copper nanocomposites using a molecular-level mixing process, Adv. Mater. 25 (2013) 6724–6729, https://doi.org/10.1002/adma.201302495
[5] L. Tsetseris, S.T. Pantelides, Graphene: an impermeable or selectively permeable membrane for atomic species, Carbon 67 (2014) 58–63, https://doi.org/10.1016/j.carbon.2013.09.055
[6] S. Shu, Q. Yuan, W. Dai, M. Wu, D. Dai, K. Yang, B. Wang, C. Te Lin, T. Wuebben, J. Degenhardt, C. Regula, R. Wilken, N. Jiang, J. Ihde, In-situ synthesis of graphene-like carbon encapsulated copper particles for reinforcing copper matrix composites, Mater. Des. 203 (2021) 109586, https://doi.org/10.1016/j.matdes.2021.109586
[7] X. Zhang, Y. Xu, M. Wang, E. Liu, N. Zhao, C. Shi, D. Lin, F. Zhu, C. He, A powder-metallurgy-based strategy toward three-dimensional graphene-like network for reinforcing copper matrix composites, Nat. Commun. 11 (2020) 2775, https://doi.org/10.1038/s41467-020-16490-4
[8] J. Rafiee, X. Mi, H. Gullapalli, A.V. Thomas, F. Yavari, Y. Shi, P.M. Ajayan, N.A. Koratkar, Wetting transparency of graphene, Nat. Mater. 11 (2012) 217–222, https://doi.org/10.1038/nmat3228
[9] X. Zhang, C. Shi, E. Liu, N. Zhao, C. He, Effect of interface structure on the mechanical properties of graphene nanosheets reinforced copper matrix composites, ACS Appl. Mater. Interfaces 10 (2018) 37586–37601, https://doi.org/10.1021/acsami.8b09799
[10] S. Das, D. Lahiri, D.Y. Lee, A. Agarwal, W. Choi, Measurements of the adhesion energy of graphene to metallic substrates, Carbon 59 (2013) 121–129, https://doi.org/10.1016/j.carbon.2013.02.063
[11] Z. Dong, Y. Peng, X. Zhang, D.B. Xiong, Plasma assisted milling treatment for improving mechanical and electrical properties of in-situ grown graphene/copper composites, Compos. Commun. 24 (2021) 100619, https://doi.org/10.1016/j.coco.2020.100619
[12] X. Li, S. Yan, X. Chen, Q. Hong, N. Wang, Microstructure and mechanical properties of graphene-reinforced copper matrix composites prepared by in-situ CVD, ball-milling, and spark plasma sintering, J. Alloy. Compd. 834 (2020) 155182, https://doi.org/10.1016/j.jallcom.2020.155182
[13] D. Zhang, Z. Zhan, Preparation of graphene nanoplatelets-copper composites by a modified semi-powder method and their mechanical properties, J. Alloy. Compd. 658 (2016) 663–671, https://doi.org/10.1016/j.jallcom.2015.10.252
[14] K. Cheng, W. Xiong, Y. Li, L. Hao, C. Yan, Z. Li, Z. Liu, Y. Wang, K. Essa, L. Lee, X. Gong, T. Peijs, In-situ deposition of three-dimensional graphene on selective laser melted copper scaffolds for high performance applications, Compos. Part A: Appl. Sci. Manuf. 135 (2020) 105904, https://doi.org/10.1016/j.compositesa.2020.105904
[15] S. Li, B. Hou, D. Dai, S. Shu, M. Wu, A. Li, Y. Han, Z. xiang Zhu, B. an Chen, Y. Ding, Q. Zhang, Q. Wang, N. Jiang, C. Te Lin, CVD synthesis of monodisperse graphene/Cu microparticles with high corrosion resistance in Cu etchant, Materials 11 (2018) 1459, https://doi.org/10.3390/ma11081459
[16] A. Dadkhah Tehrani, B. Efafi, M.H.Majles Ara, Preparing a new class of ultrathin graphene nanostructure by chemical vapor deposition and its lasing ability, ACS

Appl. Mater. Interfaces 12 (2020) 46429–46438, https://doi.org/10.1021/acsami.0c11346
[17] Z. Yang, L. Wang, Y. Cui, Z. Shi, M. Wang, W. Fei, High strength and ductility of graphene-like carbon nanosheet/copper composites fabricated directly from commercial oleic acid coated copper powders, Nanoscale 10 (2018) 16990–16995, https://doi.org/10.1039/c8nr04451a
[18] S. Wang, S. Han, G. Xin, J. Lin, R. Wei, J. Lian, K. Sun, X. Zu, Q. Yu, High-quality graphene directly grown on Cu nanoparticles for Cu-graphene nanocomposites, Mater. Des. 139 (2018) 181–187, https://doi.org/10.1016/j.matdes.2017.11.010
[19] N. Reckinger, M. Casa, J.E. Scheerder, W. Keijers, M. Paillet, J.R. Huntzinger, E. Haye, A. Felten, J. Van De Vondel, M. Sarno, L. Henrard, J.F. Colomer, Restoring self-limited growth of single-layer graphene on copper foil: Via backside coating, Nanoscale 11 (2019) 5094–5101, https://doi.org/10.1039/c8nr09841g
[20] Z.J. Wang, F. Ding, G. Eres, M. Antonietti, R. Schloegl, M.G. Willinger, Formation mechanism, growth kinetics, and stability limits of graphene adlayers in metal-catalyzed CVD growth, Adv. Mater. Interfaces 5 (2018) 1800255, https://doi.org/10.1002/admi.201800255
[21] M. Wu, B. Hou, S. Shu, A. Li, Q. Geng, H. Li, Y. Shi, M. Yang, S. Du, J.Q. Wang, S. Liao, N. Jiang, D. Dai, C. Te Lin, High oxidation resistance of CVD graphene-reinforced copper matrix composites, Nanomaterials 9 (2019) 498, https://doi.org/10.3390/nano9040498
[22] Y. Liu, C. Liang, A. Wei, Y. Jiang, Q. Tian, Y. Wu, Z. Xu, Y. Li, F. Guo, Q. Yang, W. Gao, H. Wang, C. Gao, Solder-free electrical Joule welding of macroscopic graphene assemblies, Mater. Today Nano 3 (2018) 1–8, https://doi.org/10.1016/j.mtnano.2018.09.005
[23] Y. Zhang, D. Li, X. Tan, B. Zhang, X. Ruan, H. Liu, C. Pan, L. Liao, T. Zhai, Y. Bando, S. Chen, W. Cai, R.S. Ruoff, High quality graphene sheets from graphene oxide by hot-pressing, Carbon 54 (2013) 143–148, https://doi.org/10.1016/j.carbon.2012.11.012
[24] A. Nieto, D. Lahiri, A. Agarwal, Synthesis and properties of bulk graphene nanoplatelets consolidated by spark plasma sintering, Carbon 50 (2012) 4068–4077, https://doi.org/10.1016/j.carbon.2012.04.054
[25] C. Zhang, R. Tu, M. Dong, J. Li, M. Yang, Q. Li, J. Shi, H. Li, H. Ohmori, S. Zhang, L. Zhang, T. Goto, Growth of umbrella-like millimeter-scale single-crystalline graphene on liquid copper, Carbon 150 (2019) 356–362, https://doi.org/10.1016/j.carbon.2019.05.013
[26] U. Lee, Y. Han, S. Lee, J.S. Kim, Y.H. Lee, U.J. Kim, H. Son, Time evolution studies on strain and doping of graphene grown on a copper substrate using Raman spectroscopy, ACS Nano 14 (2020) 919–926, https://doi.org/10.1021/acsnano.9b08205
[27] Y. Kim, J. Lee, M.S. Yeom, J.W. Shin, H. Kim, Y. Cui, J.W. Kysar, J. Hone, Y. Jung, S. Jeon, S.M. Han, Strengthening effect of single-atomic-layer graphene in metal-graphene nanolayered composites, Nat. Commun. 4 (2013) 1–7, https://doi.org/10.1038/ncomms3114
[28] M.R. Akbarpour, H. Mousa Mirabad, S. Alipour, Microstructural and mechanical characteristics of hybrid SiC/Cu composites with nano- and micro-sized SiC particles, Ceram. Int. 45 (2019) 3276–3283, https://doi.org/10.1016/j.ceramint.2018.10.235
[29] K. Chu, F. Wang, Y. biao Li, X. hu Wang, D. jian Huang, H. Zhang, Interface structure and strengthening behavior of graphene/CuCr composites, Carbon 133 (2018) 127–139, https://doi.org/10.1016/j.carbon.2018.03.018
[30] D.H. Xia, S. Song, L. Tao, Z. Qin, Z. Wu, Z. Gao, J. Wang, W. Hu, Y. Behnamian, J.L. Luo, Review-material degradation assessed by digital image processing: Fundamentals, progresses, and challenges, J. Mater. Sci. Technol. 53 (2020) 146–162, https://doi.org/10.1016/j.jmst.2020.04.033
[31] J.K. Chang, W.H. Lin, J.I. Taur, T.H. Chen, G.K. Liao, T.W. Pi, M.H. Chen, C.I. Wu, Graphene anodes and cathodes: tuning the work function of graphene by nearly 2 eV with an aqueous intercalation process, ACS Appl. Mater. Interfaces 7 (2015) 17155–17161, https://doi.org/10.1021/acsami.5b03934
[32] L. Dong, W. Chen, N. Deng, J. Song, J. Wang, Investigation on arc erosion behaviors and mechanism of W70Cu30 electrical contact materials adding graphene, J. Alloy. Compd. 696 (2017) 923–930, https://doi.org/10.1016/j.jallcom.2016.12.044
[33] S.M. Song, J.K. Park, O.J. Sul, B.J. Cho, Determination of work function of graphene under a metal electrode and its role in contact resistance, Nano Lett. 12 (2012) 3887–3892, https://doi.org/10.1021/nl300266p
[34] M. Xue, W. Wang, F. Wang, J. Ou, C. Li, W. Li, Understanding of the correlation between work function and surface morphology of metals and alloys, J. Alloy. Compd. 577 (2013) 1–5, https://doi.org/10.1016/j.jallcom.2013.04.113